P11.5 **STATISTICAL ASSESSMENT OF EXPLICIT MODEL FORECASTS OF CONVECTION USING A NEW OBJECT-BASED APPROACH**

C. Phillips*, J. Pinto, M. Steiner, R. Rasmussen, N. Oien and R. Bateman

NCAR/ Research Applications Laboratory

Boulder, Colorado, USA

1. INTRODUCTION

The degree to which thunderstorms affect air traffic is related to their intensity, coverage, spacing, orientation, organization and echo top heights. Aviation generally tries to avoid flying through storms with radar echoes exceeding 35 dBZ. Accurate forecasts of the most likely areas where these storms will form and the characteristics of these storm regions (coverage, spacing, etc) at lead times of 6-12 hours can greatly improve the efficiency of the National Airspace System (NAS).

Computer processor speed and memory have increased to the point such that numerical weather prediction at 4 km resolution or less can be made in real-time. At these resolutions, it is now possible to at least partially resolve convection (e.g., Weisman et al. 1997), thus eliminating the need for convective parameterizations.

As model resolution improves, new techniques for validating discrete fields such as precipitation are needed. Pixel-by-pixel verification approaches such as critical success index (CSI) and root mean squared error (RMSE) do not provide relevant information about forecast quality for many applications. Toward this end Davis et al. (2006) report on the use of an object-based approach to analyze high resolution precipitation fields. They performed analyses on 4-km Weather Research and Forecasting (WRF) model simulations that were

* *Corresponding author address:* James Pinto, NCAR, Research Applications Laboratory, Boulder, CO 80301; e-mail: pinto@ucar.edu.

run over the central US in the summer of 2003. They found that, in general, the 4-km WRF had a positive bias in fractional area covered by large storm complexes (i.e., storms > 400 km^2) and related it to MCS over-prediction.

We employ a similar approach to compare the skill of high resolution real-time WRF and Fifth-Generation Mesoscale Meterorology (MM5) model simulations, with a focus on assessing the model's ability to simulate storm characteristics relevant to aviation planning (e.g., the spacing between storms, storm size distribution, orientation and aspect ratio), rather than traditional skill scores.

2. METHODOLOGY

In this study we assess the ability of convection-permitting simulations performed with the WRF and MM5 models to predict storm characteristics in Midwestern (hereafter, MW) region of the United States centered over Chicago (Figure 1). The southeastern US (SE), which is highlighted in yellow, was discussed in a previous study with similar analyses (Phillips et al., 2007). The model reflectivity field (computed from the modeled precipitation mass) is compared with the Weather Surveillance Radar 1988 Doppler (WSR-88D) reflectivity mosaic produced by Weather Systems, Inc (WSI). We focus on the MW region because of the range of convective storm types that occur here. Convection in the MW domain is host to a wide range of environmental conditions being frequented by frontal boundaries and often more organized convection in the form of squall lines and MCSs.

2.1 Model Descriptions

In this study we compare results from the WRF ARW and the RTFDDA version of MM5. Table 1 lists the parameterization packages used by each model and details are given below.

WRF

Version 2.1.2 of the Advanced Research WRF (ARW) (Skamarock et al. 2005) model was run in real-time during the summer of 2006 (June and July) through a collaborative effort between Research Applications Laboratory (RAL) and the Mesoscale and Microscale Meteorology division (MMM) at NCAR. One of the goals of this effort was to provide convection-permitting forecasts from the WRF model to the Storm Prediction Center (SPC) forecasters to aid in their product development. The model was run twice per day (initialized at 00 and 12 UTC and run out to 36 hr and 18 hr, respectively) at a convection-resolving resolution of 4 km with 34 vertical levels. The domain and forecast length of the 12 UTC simulations were reduced because of the goal of operational availability.

Initial conditions and boundary conditions were specified using the 40-km North American Mesoscale model (NAM, grid 212). Data assimilation was not performed. The model was run using Mellor-Yamada-Janjic (MYJ) Planetary Boundary Layer (PBL), WRF Single Momen (WSM)-6 category microphysics, the Noah Land-Surface Model (LSM), and Rapid Radiative Transfer Model (RRTM)/Dudhia radiation.

MM5

The Real-Time Four-Dimensional Data Assimilation (RTFDDA) version of MM5 (Xu et al., 2005) was run in real-time at a 5-km resolution during July of 2006 over the Midwest, encompassing the Chicago area and its busy air space. See Figure 1 for each of the model domains. The model used RTFDDA including radar reflectivity nudging through the latent heating term. The MM5 model is run every 3 hr starting at 02 UTC, producing a 3 hr analyses period and a 9 hr forecast. Initial and boundary conditions for the MM5 were also specified using the 40-km NAM. Dudhia simple-ice microphysics along with Medium Range Forecast model (MRF) boundary layer scheme and Noah LSM were used to run the model.

2.2 Observations

A quality controlled version of the national 2-km grid of WSR-88D radar data (Klazura and Imy 1993) that is produced by WSI is used to determine the storm characteristics. The WSI data have been averaged to 4-km resolution using a 2 X 2 filter to match the heightest resolution model grid. The WSI data (which is available every 5 min) have also been sub-sampled hourly to be coincident with the model output times.

2.3 Analysis Techniques

The modeled and observed reflectivities are all interpolated to a common grid. Here we have chosen a 4 km grid with a lat-lon regular projection as the common grid. Each lat-lon grid is then analyzed using the Thunderstorm Identification, Tracking, and Analysis (TITAN, Dixon and Wiener 1993) software developed at the NCAR for tracking and nowcasting thunderstorms. For this study, TITAN was configured to identify storms based on a reflectivity threshold (35 dBZ) and a minimum storm area (75 km^2) or length scale of 8.66 km. We chose such a small area threshold because we wanted to assess the transition from numerical noise to feature resolution in the model. TITAN produces a number of output fields that describe each storm (e.g., centroid location, storm size, cell orientation, and cell aspect ratio). These data are then statistically analyzed to describe the bulk characteristics (over hourly, daily or monthly timescales) of the storms for the MW region. TITAN can also be

used to track storms through time; however, results from this analysis will be presented elsewhere.

The analyses are performed for the aforementioned MW domain. MM5 is only available for the MW region while both WRF model runs span a much larger area. The 00 and 12 UTC forecasts from the two models are compared. Note that the MM5 runs are actually initialized 23 and 11 UTC. Hourly and monthly mean statistics are presented below.

2.4 Midwest Region Case Study for 11 July 2006

A 500 hPA trough was centered on the MW region with a stationary frontal boundary oriented east-west across the northern third of the domain. The day began with broad areas of convection or clusters of storms propagating east-northeast across the domain (1200-1600 UTC). New storms began to initiate along an old boundary in southeastern Missouri around 1630 UTC and moved east along the southern edge of the domain (Figure 2). The WRF model produces too many small storms over eastern Iowa and Illinois compared to observations, but nicely captures the larger scale features and storm structure. The storms produced by MM5 are much larger than observed and have a "blob-like" unstructured appearance.

The observed and modeled temporal variation in the number and mean size of storms in the MW region is shown in Figure 3. It is evident that the WRF model run has too many small storms while the MM5 has too few. Note that the first 2 hours of the WRF run are needed for model spin up. This is evident in the rapid changes in storm area between 13 and 14 UTC. The MM5 model does not have to spin up because it is continuously assimilating available observation including the radar reflectivity (indirectly through latent heat nudging). Both models predict an increasing number of storms between 16 and 21 UTC, while the opposite is observed. Studying the sequence of WSI radar reflectivity maps

reveals that during this time, more storms are propagating out of the domain than are forming or moving into it (Figure 2). The models on the other hand have initiated too many storms between 17 and 21 UTC resulting in an erroneous positive trend in storm number.

The two models show different trends in storm area with the WRF having a general downward trend (with number of small storms increasing) and the MM5 having an upward trend after 18 UTC. Observations indicate that the storm area is decreasing with time, consistent with the fact that storms are propagating out of the domain.

4. MONTHLY ANALYSES

In order to draw statistically-meaningful conclusions regarding the ability of the models to represent storm characteristics, we perform these analyses over the entire month of July 2006. Here again, we compare the results of the 00 and 12 UTC runs from the WRF and MM5 over the same range of valid time for the MW region.

Plots of the hourly total number of the storms and mean storm size for the entire month of July 2006 are shown in Figure 4. Both models are able to reproduce the observed diurnal cycle of storm number and area. However, the MM5 generally has too few storms and WRF has too many (Figure 4a). The mean storm area tends to be underpredicted by both models with the 00Z WRF model runs severely underpredicting the mean storm area. The mean area in the 00Z MM5 runs is initially much better than 00Z WRF (due to assimilation), but MM5's skill at predicting mean storm area decreases rapidly with leadtime. The 12Z runs handle the storm initiation period fairly well, with both models trending up in storm number and down in mean storm size as the number of small new storm cells increases. The trends in the 12Z WRF model are steeper due to its tendency to produce too many small storms in phase with daytime solar heating.

The distribution of storm sizes shown in Figure 5 indicates the MM5 model's tendency to underpredict the number of small storms (e.g., storm area < 1000 km^2) regardless of initialization time. The WRF model's skill at predicting the distribution of storm size varies as a function of forecast initialization time with a large overestimation in small storms evident in the 12Z runs. Nevertheless, the WRF generally performs better at capturing the distribution of storm sizes than MM5.

Figure 6 contains distributions of the frequency of occurrence of modeled and observed storm aspect ratios. Values that are closer to unity represent more circular storms while higher values indicate more elongated storms. The modeled distribution of aspect ratios tends to be more narrow than observed for both models, regardless of forecast initialization time. That is, the models tend to under-represent the linear nature of the storms with the MM5 plot being noticeably less broad than WRF (as one might expect given the blob-like appearance of storms in MM5). The smaller storms predicted by WRF tend to be more circular, accounting for the differences between the observations and the WRF model.

The modeled and observed distributions of storm orientations are plotted in Figure 7. Numbers between 0° and 90° represent orientations from southwest to northeast, those near 90° have an orientation from east to west, and numbers greater than 90° represent those storms that are oriented from northwest to southeast. Each of the datasets has a tendency for east-west orientation, but notice how both models exaggerate this tendency for both initialization times. The observations indicate that the storms actually tend to be oriented southwest to northeast, which is consistent with the typical orientation of fronts in the region. Neither of the models captures this feature.

5. SUMMARY/FUTURE WORK

Although the models do not perfectly forecast the exact locations of the storms, useful storm characteristics can still be ascertained from their forecasts. The models are somewhat skillful in reproducing the storm initiation phase of the diurnal cycle in terms of storm number and area. The models also do fairly well at reproducing the distribution of storm sizes for areas > 1000 km2 (30 x 30 km or 6 x 6 grid points). This finding is consistent with other work that has shown that at least 5 gridpoints are needed to minimally resolve a feature. The WRF model does much better at simulating storms down to 375 km2 than MM5 which may be related to the fact that MM5 uses a horizontal diffusion operator to reduce spurious noise.

The models had trouble predicting storm number and area overnight when elevated convection dominates. MM5 generally predicts too few storms that are too large and circular while WRF predict too many small storms in response to daytime heating. WRF performs better than MM5 in predicting the aspect ratio or organization of the storms; however, both models tend to underpredict the frequency of occurrence of elongated storms.

In the future, a complete statistical analysis of the storm coverage in both domains will be performed. We would also like to examine how each of the models performs during distinct environmental conditions (i.e. cold front, vorticity maximum, high pressure, etc.). Since the WRF is available in both of the domains, an analysis of its performance in each of the domains will be done. Most importantly, we would like to further look into why the models tended to be different from the observations and what may be changed to help improve the simulations.

6. REFERENCES

Davis, C., Brown, B., and Bullock, R., 2006: Object-based verification of precipitation forecasts. Part II: application to convective rain systems. *Mon. Wea. Rev.*, 134, 1785-1795.

Dixon, M., and G. Wiener, 1993: TITAN: Thunderstorm identification, tracking, and nowcasting – a radar-based methodology. *J. Atmos. Oceanic Tech.*, 10, 785-797.

Klazura, G.E. and D.A. Imy, 1993: A description of the initial set of analysis products available from the NEXRAD WSR-88D system. *Bull. Amer. Meteor. Soc.*, 74, 1293-1311.

Phillips, C.L., J. Pinto, M. Steiner, and R.M. Rasmussen, 2007: Evaluation of the WRF's ability to predict the coverage of air-mass thunderstorms and applications to short-term forecasting, *16th Conference on Applied Climatology,* San Antonio, TX, P4.9

Skamarock, W.C., et al. 2005: A description of the advanced research WRF Version 2. NCAR/TN-468+STR, 100 pp.

Weisman, M.L., W.C. Skamarock, and J.B. Klemp, 1997: The resolution dependence of explicitly modeled convective systems. *Mon. Wea. Rev.*, 125, 527-548.

Xu, M., N. A. Crook, Y. Liu, and R. Rasmussen, 2005: Impact of radar assimilation on storm predictions using a mesoscale model. *32nd Conference on Radar Meteorology,* Albuquerque, NM, JP1J.11
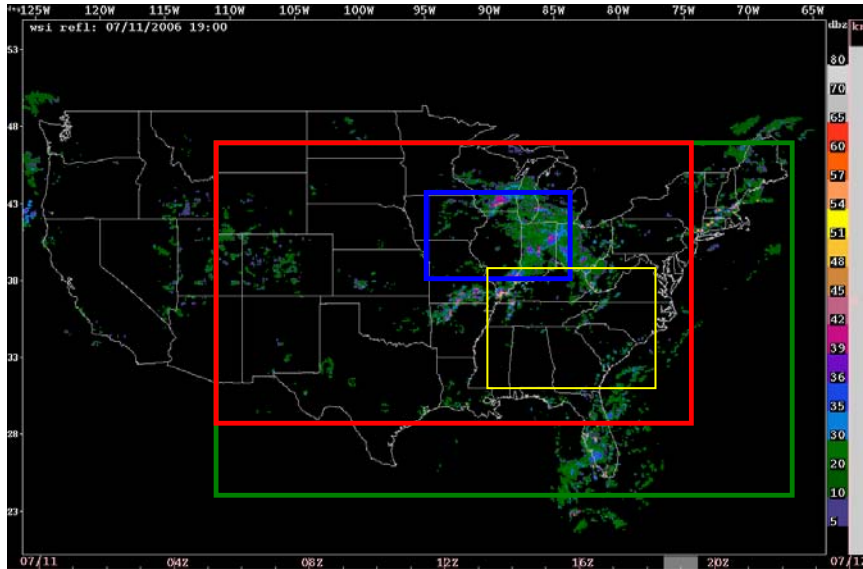
Figure 1.WSI reflectivity valid at 1900 UTC. The MM5 Domain is enclosed by the blue box. The green box is the domain over which the 00 UTC WRF runs were done, and the red box shows the domain for the 12 UTC WRF runs. Yellow box indcates the SE analysis region.

	MM5	WRF
Resolution	5 km	4 km
Microphysics	Dudhia	WSM
PBL	MRF	MYJ
LSM	Noah	Noah
BCs	40-km NAM, grid 212	40-km NAM, grid 212
Data Assimilation	3 hr	None
Convective Parameterization	None	None

Table 1. Specific parameters used with WRF and MM5 for this study.
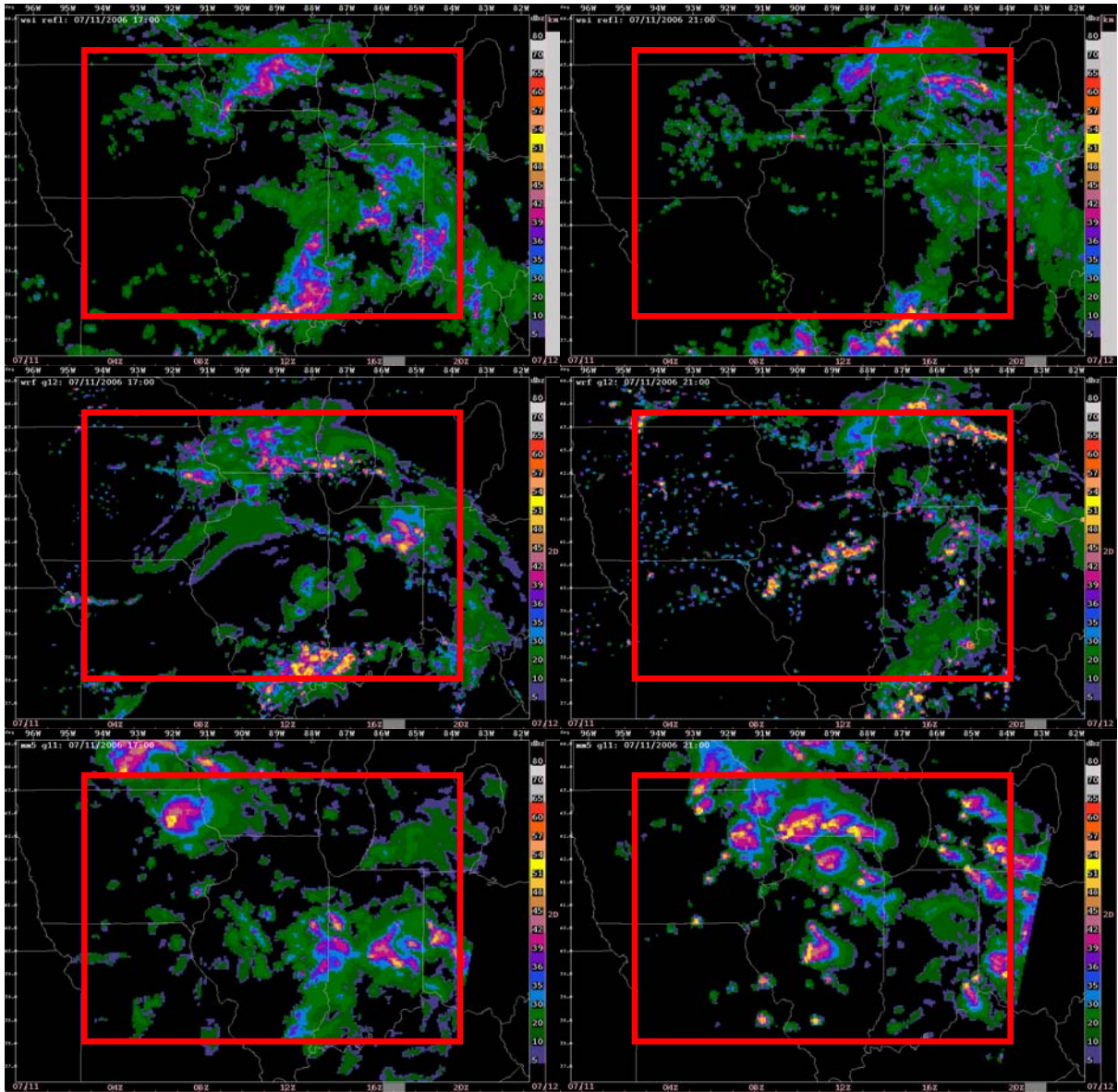
Figure 2. WSI reflectivity (top), WRF (mid), and MM5 (bottom) valid at 17 UTC (left) and 21 UTC (right) on 11 July 2006.
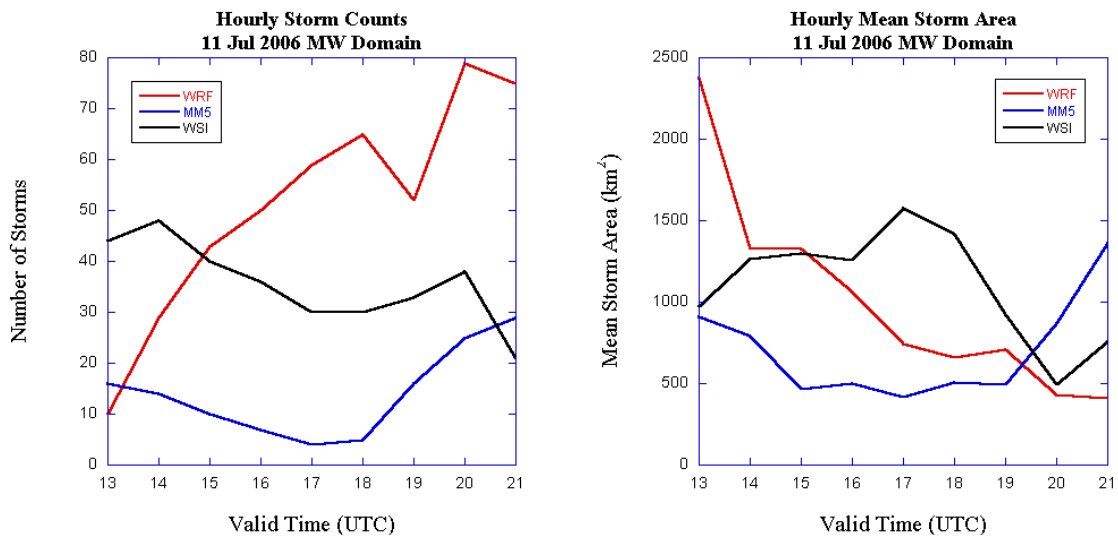
Figure 3. Plots of hourly storm counts (left) and mean storm size (right) for 11 July 2006.
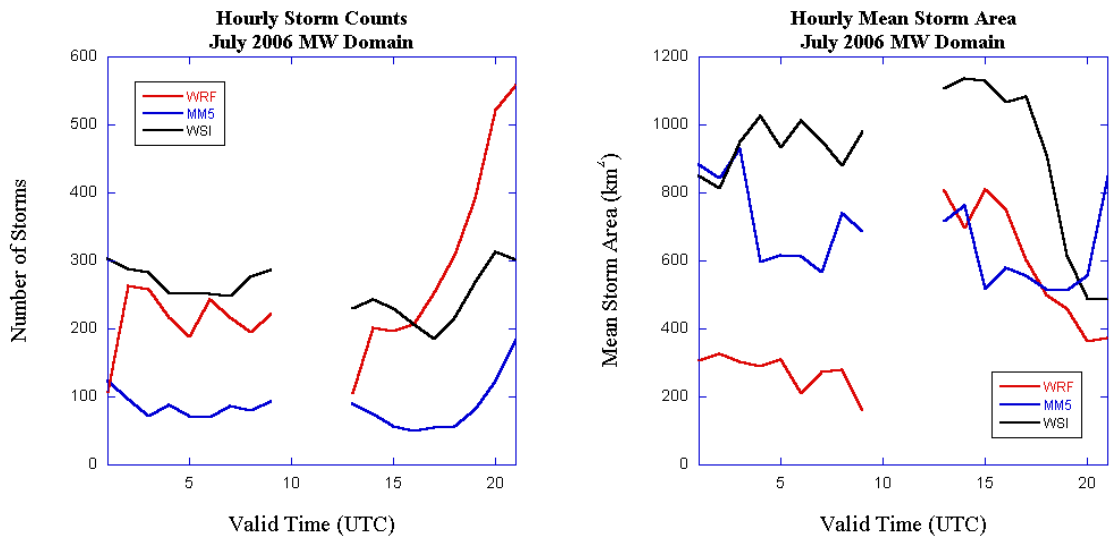
Figure 4. Plots of hourly storm counts (left) and mean storm size (right) for the entire month of July 2006. Valid times between 01 and 09 UTC and 13 and 21 UTC are plotted.
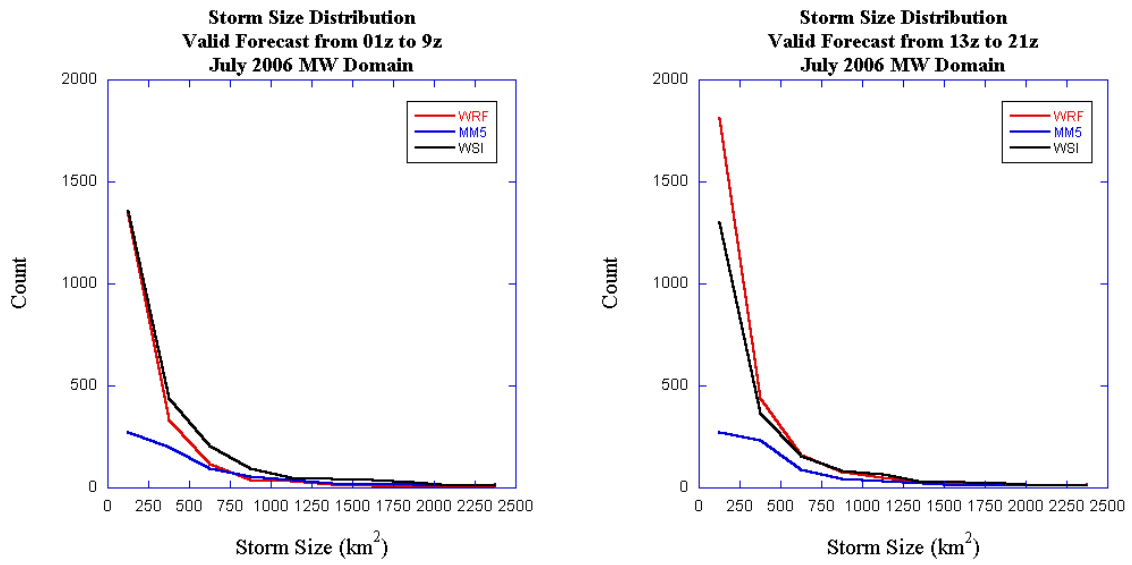
Figure 5. Storm size distributions for 00 UTC runs (left) and 12 UTC runs (right) for the entire month of July 2006.
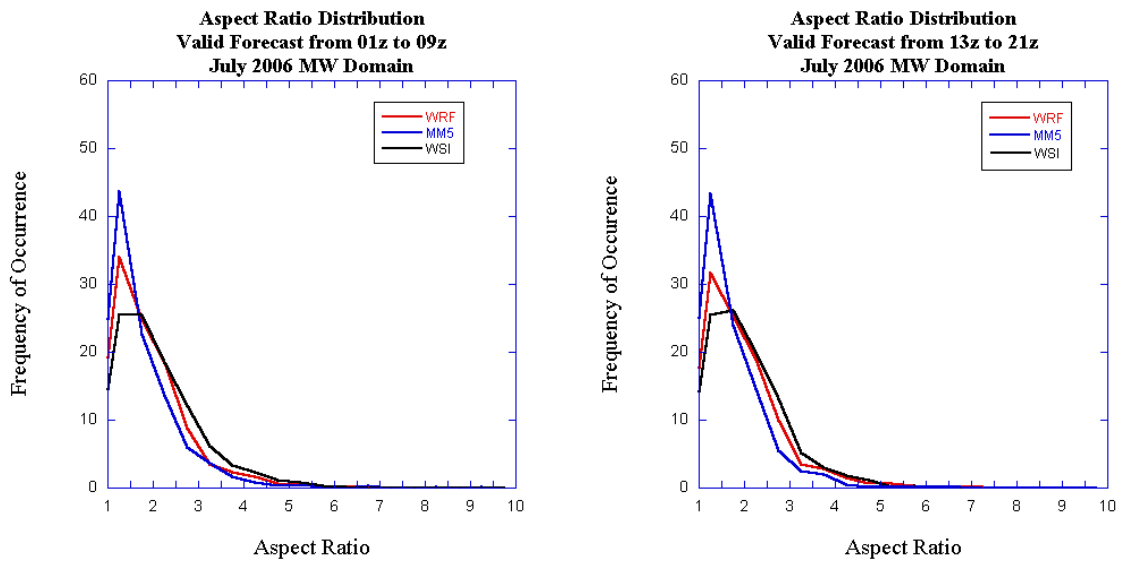
Figure 6. Distributions of the percent of forecast aspect ratios for 00 UTC runs (left) and 12 UTC runs (right) for the entire month of July 2006.
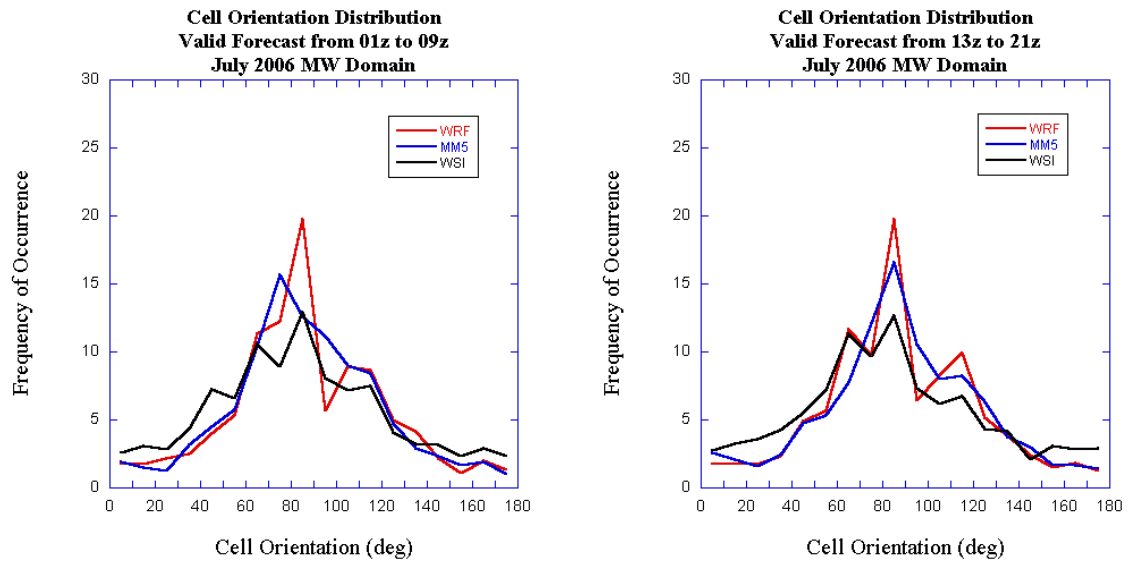
Figure 7. Distributions of the percent of forecast cell orientations for 00 UTC runs (left) and 12 UTC runs (right) for the entire month of July 2006.